EasyChair Preprint

№ 8022

Synthesis, Characterization ,Theoretical Study and Inhibitory Activity of Schiff Bases Ligands on Beta-Lactamases.

Zakia Messasma, Djouhra Aggoun and Yasmina Ouennoughi

May 22, 2022

1st International Conference on Engineering and Applied Natural Sciences

https://www.iceans.org/ May 10-13, 2022, Konya, Turkey

Synthesis, Characterization , Theoritecal study and Inhibitory Activity of Schiff bases ligands on Beta-Lactamases.

Zakia Messasma[1]*, Djouhra Aggoun[2] and Yasmina Ounoughi [3]

[1,2,3] *Laboratory of Electrochemistry, Molecular Engineering and Redox Catalysis (LEIMCR), Faculty of Technology, Ferhat ABBAS University of Setif-1, Setif 19000, A*
[1,2] *Department of Chemistry, Faculty of Sciences, Ferhat ABBAS University of Setif-1, Setif 19000, Algeria*

**(zakia.messasma@univ-setif.dz)Email of the corresponding author*

Abstract – Two Schiff bases ligands L^1 and L^2 tetradentate have been synthesized and characterized by routine physicochemical methods namely the melting temperature, solubility, molar conductance, UV-Vis spectrophotometry, IR-FT, NMR1H and NMR13C. These molecules proved to be stable, soluble in organic solvents, non-electrolytes. The structures of L^1 and L^2 and their electronic properties were calculated in the gas phase using Functional Density Theory (DFT) via the B3LYP/6-31G (d, p) method. Calculations show that the ligand L^2 is the most reactive because it has the smaller energy gap. The ligands L^1 and L^2 have been used as inhibitors against a semi-purified Beta-lactamase (BLs) and have been shown to have a significant inhibitory effect ($IC_{50} \leq 40.03$ µM), compared to the standard inhibitor, EDTA ($IC_{50} = 3.98$ mM). An overlap between their energy differences (HOMO, LUMO), their reactivities and their IC_{50}, reveals that the more the energy gap decreases, the more the reactivity increases, the more the IC_{50} decreases and the more the ligand is effective.

Keywords – Schiff bases ligands, DFT, Beta-Lactamases, Inhibition, EDTA.

I. Introduction

Extensive use of antibiotics in the past has led to the emergence of bacterial resistance among pathogenic microorganisms. Bacteria are known for their ability to adapt to the environment, and evolve into antibiotic-resistant forms by modifying their genetic makeups **[1]**. Production of detoxifying enzymes, efflux pumps, and altered receptor sites for antibiotics are some ways in which they acquire resistance. β-Lactam antibiotics account for about 60% of all antibacterial agents used to treat the infections caused by Gram-negative bacteria **[2]**. Bacteria counteract these antibiotics by acquiring the ability to produce β-lactamases, extended spectrum β-lactamases, AmpC enzymes, and metallo-β-lactamases (MBLs) **[3]**. Bacterial capability to acquire MBLs and become difficult-to-treat "superbugs" is significant [1,4]. it is well known that the Schiff base have shown a wide range of biological activities such as antifungal, antibacterial, antimalarial and enzymatic inhibition **[5]**. In light of these, we became interested to use the NNOO tetradentates Schiff bases ligands as enzyme inhibitors of Zn-MBLs which are usually extracted from *Acinetobacter baumannii*.

II. Materials and Method

A. Synthesis of Schiff bases ligands L^1 and L^2

(1mmol) of 1,2-diaminobenzene dissolved in 10 ml of ethanol (EtOH), are added 0.152 g (2 mmol) of thioacetic acid for L^1 or 0.244 g (2 mmol) of salicylaldehyde for L^2 dissolved in 8 ml of ethanol (EtOH). Each of two mixtures is stirred at 50°C

and under a nitrogen atmosphere until an brown and orange colored precipitate forms, respectively. These precipitates were then collected by filtration, washed several times with cold ethanol and then with diethylether to remove any traces of unreacted starting materials, and finally dried in a vacuum desiccator. The synthesis of the two ligands is shown in the following Scheme 1.

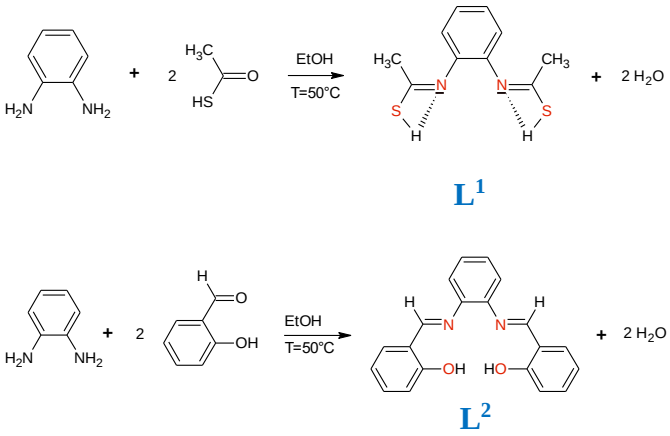

Scheme 1. Protocol for the synthesis of L^1 and L^2

B. Computational studies

The geometry optimization of ligands L^1 and L^2 was done by means of density functional theory (DFT) with a hybrid function B3LYP using the Leee Yange Parr. All the calculations were performed by Gaussian 09 suite of program at 6–31G(d,p) basis set **[6-10]**. After optimization, properties of frontier molecular orbitals (HOMO, LUMO) of L^1 and L^2 were analyzed using results calculated with the B3LYP/6–31G (d,p) method.

C. Inhibition of metallo-beta-lactamase

The purpose of this assay is to identify compounds that act as inhibitors of *Acinetobacter baumannii* MBLs. To examine this effect, an enzyme assay was performed by determining the IC_{50}, which is defined as the concentration of inhibitor necessary to inhibit 50% MBLs activity. The assay was performed at 30°C in 0.65 ml of assay buffer (50 mM HEPES ; pH 7.2 ; 50 µM $ZnSO_4$; 150 mM NaCl and 0.005 mg BSA/ml) after incubating of 10 µl semi-purified extract of metallo-betalactamases for 10 min with varied final concentrations of EDTA (1µM to 5 mM), clavulanic acid (1µM to 7 mM), and Schiff bases L^1 (1-100 µM) and L^2 (1-80 µM) and initiating the reaction with cephaloridin (80 µM) .

Percentage of Inhibition of beta-lactamase was calculated as follows:

$$\textbf{Inhibition \% = 100 x [1 –(Ac/A}_e\textbf{)]}$$

Where, A_C: metallo-betalactamase activity without inhibitors and Ae: metallo-betalactamase activity with inhibitor.

III. RESULTS

A. Physico-chemicals characterization

The main physical data of Schiff bases L^1 and L^2 are reported in **Table 1.**

Table 1. Physical data for the ligands.

Compound	**Colour**	**Yield (%)**	**R_f**	**M.p (C°)**	**Conductivity ($ohm^{-1}.cm^2.mol^{-1}$)**
L^1	Brown	42	59	260	3.79
L^2	Orange	71	82	212	8.89

B. Spectroscopic characterization

Table 2. Spectroscopic IR and UV-Vis of ligands L^1 and L^2.

Compound	**L^1**	**L^2**
Infra rouge ν (cm^{-1})		
νS-H/ νO-H	3447	3459
ν C=N	1639	1624
νC=C	1545	1607
ν C-O/ν C-S	1300	1282
UV/Vis λmax (nm) [ε] ($l.mol^{-1}$ cm^{-1})		
	280 [94 x 10^5], 398 [86.3 x 10^5]	277 [26.6 x 10^6], 336 [33 x 10^6]

C. Nuclear Magnetic Resonance Spectroscopy (NMR)

- **L^1**: **RMN ^{1}H** ($CDCl_3$, δ ppm) : 8.25 (s,1H, SH), 7.53-7.10 (m, 4H, Ar-H), 2.11 (s, 3H, CH_3).
- **L^1**: **RMN ^{13}C** ($CDCl_3$, δ ppm) : 125.20 (C1, CH=CH-CH), 126.16 (C2, CH-CH=CH), 130.25 (C3, CH=CH-N), 169,41 (C4, N=C-), 23.81 (C5, N=C-CH_3).
- **L^2** : **RMN ^{1}H** ($CDCl_3$, δ ppm) : 13.05 (s,2H,OH), 8.59 (s,1H,N=CH), 6.89-7.33, (m, Ar-H).

D. DFT Calculation

D.1. Optimized geometric structures

Molecular structures optimized with the L^1 and L^2 ligands numbering scheme are shown in **Fig.1**. The optimized geometric parameters (bond length, bond angle and dihedrals) of the title molecules calculated by DFT with B3LPY/6-31G (d, p) are listed in **Table.3**.

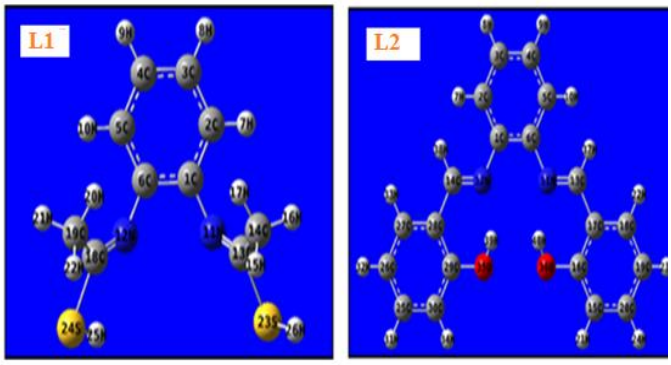

Fig 1. Optimized structures of L^1 and L^2 with atom numbering calculated from the B3LYP/6-31G method (d, p).

Table.3. The calculated structural parameters of the ligands L^1 and L^2.

L^1

Bond length (Å)		Bond angles (°)		Dihedral angles (°)	
C1-C6	1,4034	C2-C1-H7	120,8976	C6-C1-C2-H8	-179,2622
C1-N11	1,4106	C3-C4-H10	120,9005	C1-C2-C3-C4	-0,0648
C6-N12	1,4106	C5-C4-H10	117,949	C1-C2-C3-H9	179,9446
N11-C13	1,2731	C4-C5-N11	118,4036	H8-C2-C3-H9	-0,0355
N12-C18	1,2731	C6-C5-N11	122,409	C2-C3-C4-C5	0,747
C13-C14	1,5097	C1-C6-C5	119,0244	C2-C3-C4-H10	-179,521
C13-S23	1,798	C1-C6-N12	118,4005	H9-C3-C4-C5	-179,2623
C14-H17	1,0951	C5-C6-N12	122,4147	H9-C3-C4-H10	0,4696
C18-C19	1,5097	C5-N11-C13	122,5117	H10-C4-C5-C6	178,1883
C18-S24	1,798	C6-N12-C18	122,5053	H10-C4-C5-N11	2,658
C19-H20	1,0951	N11-C13-C14	128,0329	C3-C4-H10-H15	-132,6618
C19-H21	1,0915	N11-C13-S23	114,3995	C5-C4-H10-H15	47,0785
S23-H26	1,3476	C14-C13-S23	117,5661	C4-C5-C6-C1	2,6996
S24-H25	1,3476	C13-C14-H16	111,0622	N11-C5-C6-C1	178,0423
		C13-C14-H17	109,8229	N11-C5-C6-N12	-6,6377
		C12-C18-S24	114,3963	C4-H10-H15-C14	-122,9893
		C19-C18-S24	117,58	C5-N11-C13-C14	2,2477
		C13-S23-H26	97,1669	S23-C13-C14-H16	-42,8818
		C18-S24-H25	97,1695	S23-C13-C14-H17	77,2911

L^2

Bond length (Å)		Bond angles (°)		Dihedral angles (°)	
C1-C6	1.4182	C1-C2-H7	118.8083	C6-C1-C2-C3	-0.352
C1-N12	1.4035	C4-C5-H10	120.0893	C6-C1-C2-H7	177.3594
C6-N11	1.4035	C1-C6-C5	119.083	N12-C1-C2-C3	-178.7177
C2-H7	1.0844	C1-C6-N11	118.7124	N12-C1-C2-H7	-1.0062
N11-C13	1.2931	C6- N11-C13	120,7287	C2-C1-C6-C5	0.0086
N12-C14	1.2931	C1-N11-C14	120.7307	C2-C1-C6-N11	-178.412
C13-C17	1.4478	N11-C13-C17	122,5096	N12-C1-C6-N11	0.011
C13-H37	1.0981	N11-C13-H37	120,8084	C2-C1-N12-C14	- 41.2039
C14-H38	1.0981	C17-C13-H37	116.618	C6-C1-N12-C14	140.4246
C14-C28	1.4478	N12-C14-H38	120.8719	N11-C13-C17-C16	1.0117
C16-O36	1.3383	C28-C14-H38	116.6157	N11-C13-C17-C18	179.061
C29-O35	1.3383	C16-O36-H40	107.4526	H37-C13-C17-C16	-179.709
O35-H39	0.9954	C29-O35-H39	107.4579	N12-C14-C28-C29	-1.012
O36-H40	0.9954			H21-C15-C16-O36	-0.0515
				C15-C16-O36-H40	178.9432
				C28-C29-O35-H39	1.1407
				C30-C29-O35-H39	-178.9247

D.2. Frontier Molecular Orbital (FMO) Analysis

HOMO and LUMO are called Frontier Molecular Orbitals (FMO), which have played an important role in evaluating the molecular chemical stability, chemical reactivity and hardness/softness of the molecule. HOMO and LUMO energy, energy gap, ionization potential (I), electron affinity (A), electronegativity (χ), electronic chemical potential (μ), chemical hardness (η), degree of molecular softness (S) and the electrophilicity index (ω) are listed in Table 4.

Table 4. Comparison of HOMO, LUMO, energy gap (HOMO-LUMO) and associated molecular properties of L^1 and L^2 (a.u).

Molecular energy	L^1	L^2
Ionization Potential **(I)**	0.20830	0.20862
Electronic Affinity **(A)**	0.03147	0.06530
electronic chemical potential **(μ)**	-0.11572	-0.13711
Electronegativity **(χ)**	0.11572	0.13711
Chemical Hardness **(η)**	0.09257	0.07181
Softness **(S)**	5.40131	6.96281
Electrophilicity Index **(ω)**	0.07232	0.13089
E_{HOMO}	-0.20830	-0.20862
E_{HOMO-1}	-0.23163	-0.21687
E_{LUMO}	-0.02314	-0.06530
E_{LUMO+1}	-0.02041	-0.05720
E_{HOMO}-E_{LUMO}	0.18516	0.14362
E_{HOMO-1}- E_{LUMO+1}	0.20236	0.16150

The electron density distribution of the two ligands is shown in **Fig. 2**.

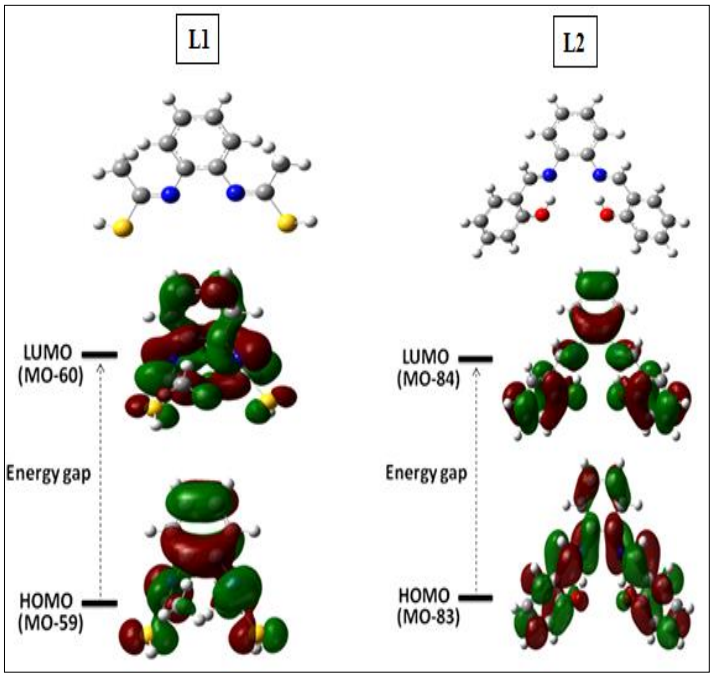

Fig.2. Diagrams of the HOMO, LUMO orbitals of the ligands L^1 and L^2 obtained with the DFT-B3LYP/6-31G method (d, p).

D.3. Molecular electrostatic potential analysis (MEP)

For this purpose, molecular electrostatic potentials (MEPs) were calculated for L^1 and L^2 at the B3LYP/6-31G level (d, p). In MEP plots, the total electron density mapped with an electrostatic

potential surface of the ligands is shown in **Fig. 3A, 3B and 3C.**

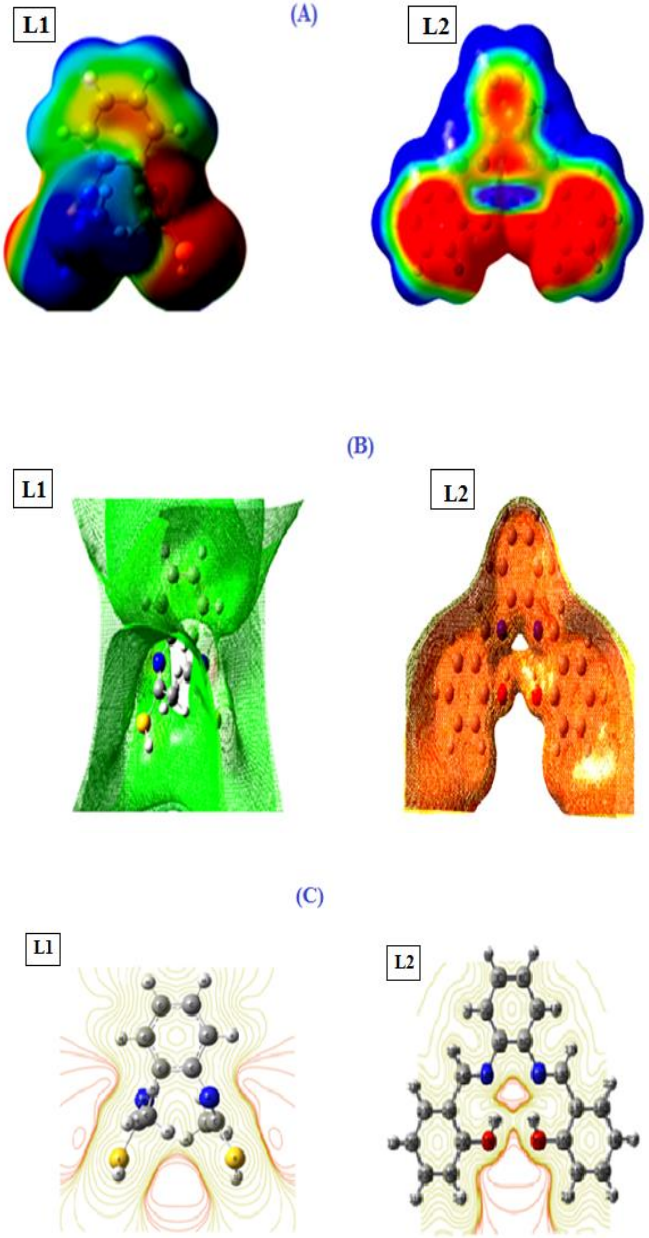

Fig.3. (A) The total electron density surface mapped with the electrostatic potential (EMP) plot of L^1 and L^2. Isovalue = 0.0004. Computing level: B3LYP/6-31G (d,p); **(B)** The electrostatic potential surface and **(C)** the electrostatic potential contour map of L^1 and L^2.

E. Inhibition activity of Schiff base ligands on MBLs

The saturation curves of L^1 and L^2 is shown in **Fig. 4**

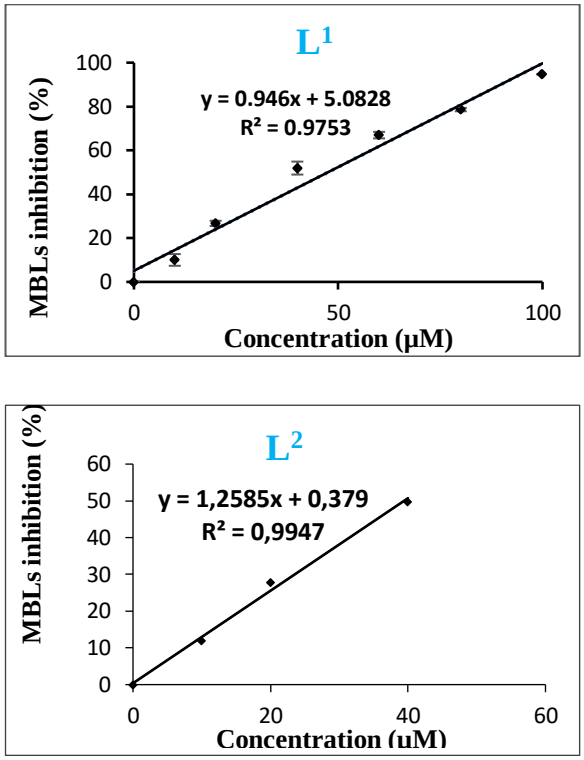

Fig 4. Saturation curves plotted against increasing concentrations of Schiff base ligands and percentage inhibition of semi-purified MBL extract.

The IC_{50} values calculated from logit-log curves (**Fig.5**)

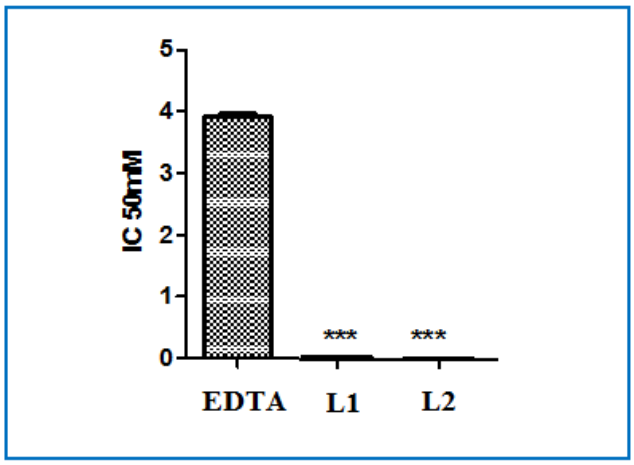

Fig.5. The IC_{50} values of L^1, L^2 and EDTA ligands from the activity of the semi-purified extract of beta-lactamases. Results expressed as means ± standard deviation (n = 3). Statistical significance of difference from corresponding values of control incubations: ***P<0.001.

IV. DISCUSSION

according to the results of **table 1**, L^1 and L^2 ligands occur as brown crystals and orange powder, respectively. These compounds, obtained

with fairly good yields, characterized by their melting points which are in agreement with those reported in the literature **[11]**. They are quite stable at room temperature and can be stored for a long period. Molar conductivity values are low. They show that solutions of Schiff base ligands are not electrolytes **[12].**

Concerning the results of the IR shown in **Table 2**, The valence vibrations (stretchings) of the hydroxyl groups (O-H) and of the thiol groups (S-H) are observed in the interval 3000-3500 cm^{-1}, these bands are wide because of the intramolecular interactions between the hydrogen of the hydroxyl or sulfur and nitrogen (OH---N or SH---N). Indeed, the frequencies of the valence vibration of the imine or azomethine double bonds (C=N) are around 1600 cm^{-1} **[13,14].**

The 1H NMR spectra of two ligands L^1 and L^2 in CDC13 showed that aromatic protons were multiplets in the range of 7.53–7.10 ppm in ligand L^1. In The L^1 ligand, SH protons appear as clusters of sharp singlets at 8.25. The chemical shifts obtained for the hydrogen atoms of the methyl groups are quite small. All values are ≤ 3 ppm **[15]** δ = 2.11 and δ = 2 ppm corresponding to methyl protons (CH_3) for L^1. For 13C NMR, the L^1 ligand, the C1, C2 and C3 signals (benzene carbons) are observed respectively at 125,200, 126,163 and 130,254 ppm, the C5 signal of L^1, is observed at 23,811 ppm. The formation of the Schiff base is supported by the presence of a corresponding C4 peak for L^1 (azomethine carbon) at 169.411 ppm.

While the DFT Calculations, geometry optimization shows that, C-C bond distances are in the range of 1.391–1.5399 Å for both ligands, while for C=N these values are 1.2731 Å for L^1 and 1.2931 Å for L^2. In the case of C-H bond distances, they are in the range of 1.081 to 1.091 A° and 1.0488 to 1.0981 A°, for L^1 and L^2, respectively. The S-H bond is at 1.347 A° for L^1 while the O-H bond is at 0.9954 A° for L^2. . The N-C-C angle in L^1 and L^2 is approximately the same at 125° and also for the N-C-S angle at 114.6°. All dihedrals of four molecules are close to -179 or +180 (**see Table.3**).

In our work, L^1 has a larger energy gap than L^2. The energy deficit (E_{HOMO} - E_{LUMO}) intervenes directly in the hardness/softness of a chemical species. A larger energy space value represents more hardness or less flexibility of a compound; thus, L^1 is called a hard molecule and the order of stability is: L^1 (0.09257 a.u) > L^2 (0.07181a.u).
The chemical potential of the global reactivity descriptor (I), represented by the HOMO energy, arises from the distribution of charges between two systems having different chemical potentials. The ionization potential (I) of L^1 and L^2 are 0.20830 and 0.208620 a.u, respectively, as shown in Table 4, which clearly indicates that the L^1 ligand has a greater tendency to donate electrons than the L^2 ligand. Another electrophilicity index of the global reactivity descriptor (ω) describes the electron acceptability of systems quite similar to (η) and (I). High values of the electrophilicity index increase the electron accepting abilities of molecules. Thus, the L^1 ligand is found to be the strongest nucleophile, while the L^1 ligand is the strongest electrophile. The values of the electronic chemical potential for the two Schiff bases are presented in Table 4. The largest electronic chemical potential (absolute values) is the least stable or the most reactive. The trend of the electronic chemical potential is $|\mu L^2| > |\mu L1|$.

As shown in **Fig 3A** and **3C**, negative regions represented by red color are preferable sites for electrophilic attack, and positive regions represented by blue color are favorable sites for nucleophilic attack. Here the negative potentials are generated on the electronegative oxygen or sulfur atoms O34, O35, O36, S23 and S24 and the nitrogen atoms N3, N4, N10, N11 and N12 while the H atoms have a region of positive potential in structures. These negative and positive sites predict the regions in a compound responsible for non-covalent interactions **[16].**

The saturation curves obtained (**Fig.4**) show that our Schiff base ligands inhibit the hydrolytic activity of our enzymatic extract in a dose-dependent manner. The IC_{50} values calculated from the logit-log curves are respectively: 3.98 mM, 33.35 ± 1.00 and 40.03 ± 1.00 µM . These values show that these inhibitions are all significant compared to the classic inhibitor, EDTA (**Fig. 5**).

V. CONCLUSION

In this work we have synthesized and characterized two Schiff base ligands (L^1 and L^2). The two

ligands proved to possess good inhibitory activity against MBLs because they exert this inhibition at concentrations of tens of micromolars. The L^2 ligand (IC_{50} = 33.35 ± 1.00 µM) is more active than the other ligand (IC_{50} = 40.03 ± 1.00 µM µM). Molecular structures were optimized by DFT using the 6-31G method (d,p). After optimization, the molecular electrostatic potential (MEP) and the properties of the frontier molecular orbitals (HOMO, LUMO) were determined. The results obtained indicate that the L^2 ligand, with a smaller energy difference (HOMO, LUMO), is more flexible, less stable, more electrophilic and more reactive than the ligand L^1. From the theoretical calculations carried out for these ligands, it can be concluded that their electronic properties correlate well with their inhibitory activities of MBLs quantified by the IC_{50} parameter, i.e. the more the reactivity of the ligand increases, the more this parameter decreases.

ACKNOWLEDGMENT

The authors thank the Algerian Ministry of Higher Education and Scientific Research (MESRS) and the General Directorate for Scientific Research and Technological Development (DGRSDT) for the financial support

REFERENCES

[1] M. A. Toleman,. P. M. Bennett, , and T. R Walsh, ISCR elements: novel gene-capturing systems of the 21st century Microbiol. Mol. Biol. Rev. 70, (2006) 296–316.

[2] D. M..Livermore and N. Woodford, The β-lactamase threat in Enterobacteriaceae, Pseudomonas and Acinetobacter. Trends Microbiol. 14, (2006) 413–420.

[3] A. Carattoli, Resistance plasmid families in Enterobacteriaceae. Antimicrob. Agents Chemother. 53, (2009). 2227–2238.

[4] J. A. Patzer, T. R.Walsh, J. Weeks, D..Dzierzanowska,and M. A. Toleman, Emergence and persistence of integron structures harbouring VIM genes in the Children's Memorial Health Institute, Warsaw, Poland, (2009) 1998-2006.

[5] L. Puccetti, G. Fasolis, D. Vullo, Z.H. Chohan, A. Scozzafava, C.T. Supuran, Carbonic anhydrase inhibitors. Inhibition of cytosolic/tumor-associated carbonic anhydrase isozymes I, II, IX, and XII with Schiff bases incorporating chromone and aromatic sulfonamide moieties, and their zinc complexes, Bioorg. Med. Chem. Lett. 15 (2005) 3096–3101

[6] D.B. Axel, Density functional thermochemistry. III. The role of exact exchange, J. Chem. Phys. 98 (1993) 5648–5652.

[7] M.J. Frisch, G.W. Trucks, H.B. Schlegel, G.E. Scuseria, M.A. Robb, J.R. Cheeseman, G. Scalmani, V. Barone, B. Mennucci, G.A. Petersson, H. Nakatsuji, M. Caricato, X. Li, H.P. Hratchian, A.F. Izmaylov, J. Bloino, G. Zheng, J.L. Sonnenberg, M. Hada, M. Ehara, K. Toyota, R. Fukuda, J. Hasegawa, M. Ishida, T. Nakajima, Y. Honda, O. Kitao, H. Nakai, T. Vreven, A J, Jr. Montgomery, J.E. Peralta, F. Ogliaro, M. Bearpark, J.J. Heyd, E. Brothers, K.N. Kudin, V.N. Staroverov, R. Kobayashi, J. Normand, K. Raghavachari, A. Rendell, J.C. Burant, S.S. Iyengar, J. Tomasi, M. Cossi, N. Rega, J.M. Millam, M. Klene, J.E. Knox, J.B. Cross, V. Bakken, C. Adamo, J. Jaramillo, R. Gomperts, R.E. Stratmann, O. Yazyev, A.J. Austin, R. Cammi, C. Pomelli, J.W. Ochterski, R.L. Martin, K. Morokuma, V.G. Zakrzewski, G.A. Voth, P. Salvador, J.J. Dannenberg, S. Dapprich, A.D. Daniels, Ö. Farkas, J.B. Foresman, J.V. Ortiz, J. Cioslowski, D.J. Fox, Gaussian 09, Revision A.02, Gaussian, Inc., Wallingford CT, 2009.

[8] G. Nidhi, P.S. Udai, Syntheses, structural, computational, and thermal analysis of acid–base complexes of picric acid with n-heterocyclic bases, J. Phys. Chem. A 117 (2013) 10428–10437.

[9] N. Goel, N. Kumar, Study of supramolecular frameworks having aliphatic dicarboxylic acids, N,N-bis(salicyl)ethylenediamine and N,N-bis(salicyl)butylenediamine, J. Mol. Sruct. 1071 (2014) 60–70.

[10] L. Chengteh, Y. Weitao, G.P. Robert, Development of the Colle-Salvetti correlation-energy formula into a functional of the electron density, Phys. Rev. 37 (1988) 785–789

[11] H. Yin, L. Xu, N.A. Porter, Free radical lipid peroxidation: mechanisms and analysis, Chem. Rev. 111 (2011) 5944–5972.

[12] S. Murtaza, M.S. Akhtar, F. Kanwal, A. Abbas, S. Ashiq, S. Shamim, Synthesis and biological evaluation of Schiff bases of 4-aminophenazone as an anti-inflammatory, analgesic and antipyretic agent, J. Saudi Chem. Soc. 21 (2017) S359–S372

[13] V. Reddy, N. Patil, S. D. Angadi, Synthesis, characterization and antimicrobial activity of Cu (II), Co (II) and Ni (II) complexes with O, N, and S donor ligands, *E-J. Chem.* **5** (2008) 577.

[14] K. Nakamato, Infrard Spectra of inorganic and coordination Compounds, John Wiley,New York, (1970).

[15] F.A. Cotton, C.W. Wilkinson, Advanced Inorganic Chemistry, 3rd ed., Interscience publisher, New York, (1972) 431.

[16] Ebrahimipour, S.Y. Abaszadeh, M. Castro, J. Seifi, Synthesis, X-ray crystal structure, DFT calculation and catalytic activity of two new oxido-vanadium (V) complexes containingONO tridentate Schiff bases, *Polyhedron*. 79 (2014) 138-150.